

## Electrohydrodynamic stability of a plasma-liquid interface

J. T. Holgate, M. Coppins, and J. E. Allen

Citation: *Appl. Phys. Lett.* **112**, 024101 (2018);

View online: <https://doi.org/10.1063/1.5013934>

View Table of Contents: <http://aip.scitation.org/toc/apl/112/2>

Published by the [American Institute of Physics](#)

---

### Articles you may be interested in

[Compressive response and deformation mechanisms of vertically aligned helical carbon nanotube forests](#)  
*Applied Physics Letters* **112**, 021902 (2018); 10.1063/1.5008983

[The transmission spectrum of sound through a phononic crystal subjected to liquid flow](#)  
*Applied Physics Letters* **112**, 024102 (2018); 10.1063/1.5017168

[Chiroptic response of ferroelectric liquid crystals triggered with localized surface plasmon resonance of achiral gold nanorods](#)  
*Applied Physics Letters* **112**, 021102 (2018); 10.1063/1.5005054

[Spectral tuning of optical coupling between air-mode nanobeam cavities and individual carbon nanotubes](#)  
*Applied Physics Letters* **112**, 021101 (2018); 10.1063/1.5008299

[Tunable modulation of refracted lamb wave front facilitated by adaptive elastic metasurfaces](#)  
*Applied Physics Letters* **112**, 021903 (2018); 10.1063/1.5011675

[Optical and electrical properties of the transparent conductor SrVO<sub>3</sub> without long-range crystalline order](#)  
*Applied Physics Letters* **112**, 021905 (2018); 10.1063/1.5016245

---

**Scilight**

Sharp, quick summaries **illuminating**  
the latest physics research

Sign up for **FREE!**



## Electrohydrodynamic stability of a plasma-liquid interface

J. T. Holgate,<sup>1</sup> M. Coppins,<sup>1</sup> and J. E. Allen<sup>1,2,3</sup>

<sup>1</sup>Blackett Laboratory, Imperial College London, London SW7 2BW, United Kingdom

<sup>2</sup>University College, Oxford OX1 4BH, United Kingdom

<sup>3</sup>OClAM, Mathematical Institute, Oxford OX2 6GG, United Kingdom

(Received 14 November 2017; accepted 23 December 2017; published online 8 January 2018)

Many plasma applications involve the plasma coming into contact with a liquid surface. Previous analyses of the stability of such liquid surfaces have neglected the presence of the sheath region between the bulk plasma and the liquid. Large electric fields, typically in excess of several  $\text{MV m}^{-1}$ , and strong ion flows are present in this region. This paper considers a linear perturbation analysis of a liquid-sheath interface in order to find the marginal condition for instability. This condition shows that molten metal surfaces in tokamak edge plasmas are stable against the electric field, if a normal sheath is formed, due to the impact of ions on the surface. The stabilization of the liquid surface by ion bombardment is encouraging for the ongoing development of plasma-liquid technologies. © 2018 Author(s). All article content, except where otherwise noted, is licensed under a Creative Commons Attribution (CC BY) license (<http://creativecommons.org/licenses/by/4.0/>). <https://doi.org/10.1063/1.5013934>

The study of plasma-liquid interactions is an increasingly important topic in the field of plasma science and technology with applications in nanoparticle synthesis, catalysis of chemical reactions, material processing, water treatment, sterilization, and plasma medicine.<sup>1,2</sup> This particular work is motivated by the plasma-liquid interactions inherent in magnetic confinement fusion devices, such as tokamaks, either due to melt damage of the metal walls<sup>3</sup> or in new liquid metal divertor concepts.<sup>4-6</sup> The ejection of molten droplets has been observed in both cases<sup>7,8</sup> and is of considerable concern to the operation of a successful fusion device. Understanding the stability of the liquid metal surface is a critical issue.

Previously studied instabilities of liquid metal surfaces in tokamaks include a Kelvin-Helmholtz instability due to plasma flow across the metal surface,<sup>9</sup> a Rayleigh-Taylor instability driven by the  $j \times B$  force due to a current flowing in the metal,<sup>10</sup> a Rayleigh-Plateau instability of the liquid metal rim around a cathode arc spot crater,<sup>11</sup> and droplet emission from bursting bubbles which are formed by liquid boiling or absorption of gases from the plasma.<sup>12</sup> However, none of these studies considers the effect of the strong electric fields and ion flows in the sheath region between the plasma and the liquid surface despite the observations of electrical effects such as arcing, which cause considerable damage to the tokamak wall,<sup>13</sup> and enhanced droplet emission rates from electrically biased surfaces.<sup>7</sup> Furthermore, electrostatic breakup has been identified as an important process for liquid droplets in plasmas.<sup>14</sup>

Instabilities driven by electric fields, i.e., electrohydrodynamic (EHD) instabilities, at the interface between a conducting liquid and vacuum were originally studied by Melcher<sup>15</sup> and subsequently by Taylor and McEwan.<sup>16</sup> Melcher's marginal stability criterion was invoked by Bruggeman *et al.* in order to explain the filamentary structure of a glow discharge over a water cathode<sup>17</sup> and, additionally, to explain the instability of an electrolytic water solution cathode from an earlier

experiment.<sup>18</sup> Earlier evidence for EHD instabilities of the plasma-liquid interface appears in an experiment on unrelated work<sup>19</sup> where an arc spot occasionally formed on an electrically isolated mercury pool which was in contact with the plasma. Another EHD effect, the deformation of a liquid surface into a Taylor cone, has recently been used to form the cathode of a corona discharge.<sup>20</sup>

This paper investigates the EHD stability of a plasma-liquid interface with a linear perturbation analysis. Melcher's stability criterion is found to apply to short-wavelength perturbations of the surface. However, the fast-moving ions in the sheath provide a significant pressure on the liquid surface which can overcome the electric stress for long-wavelength perturbations. This effect has been neglected in previous studies and provides an overall increase in the critical voltage which must be applied to the surface in order to make it unstable. This effect is encouraging for the ongoing development of new plasma-liquid technologies.

The interface between a plasma and a liquid, together with the intermediate sheath region, is illustrated schematically in Fig. 1. The liquid provides a sink of electrons and ions from the plasma which are drawn towards the surface and, due to the higher average speed of the electrons, give the surface a negative electric charge and hence a negative potential. The potential difference is always measured from zero at the plasma-sheath edge in this paper. The potential drop across the sheath acts to accelerate ions and repel electrons so that the electron and ion currents to the surface become balanced. This requires a large electric field which can drive EHD instabilities of the liquid surface. The situation is complicated by the ions from the plasma which, due to their impact with the surface, exert a considerable pressure on the plasma-liquid interface.

One of the simplest mathematical models of a plasma sheath is that of Bohm.<sup>21,22</sup> This comprises a collisionless cold-ion fluid, with density  $n$  and velocity  $\underline{u}$ , and Boltzmann-distributed electrons with temperature  $T_e$ . These particles

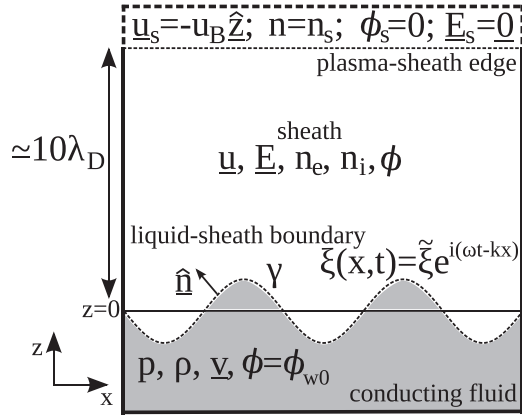


FIG. 1. Illustration of the variables throughout the plasma-sheath-liquid transition region for a negatively charged, perturbed liquid surface. The electron density is given by the Boltzmann relation,  $n_e = n_s \exp(e\phi/k_B T_e)$ , while the ion density  $n_i$  is abbreviated to  $n$  elsewhere in this paper.

interact with each other and a conducting wall via the electrostatic field  $\underline{E}$  which is described by the potential  $\phi$ . Inserting the Boltzmann relation into Poisson's equation gives the sheath equations

$$\frac{\partial n}{\partial t} + \nabla \cdot (n\underline{u}) = 0, \quad (1)$$

$$m_i \frac{\partial \underline{u}}{\partial t} + m_i (\underline{u} \cdot \nabla) \underline{u} = e\underline{E}, \quad (2)$$

$$\nabla \cdot \underline{E} = \frac{e}{\epsilon_0} \left[ n - n_s \exp\left(\frac{e\phi}{k_B T_e}\right) \right]. \quad (3)$$

The boundary conditions at the sheath-plasma edge are provided by asymptotically matching these equations with the quasineutral plasma as  $n = n_s$ ,  $\underline{E}_s = \underline{0}$ ,  $\phi_s = 0$ , and  $\underline{u}_s = -(k_B T_e/m_i)^{1/2} \underline{\hat{z}} = -u_B \underline{\hat{z}}$  in the limit  $z \rightarrow \infty$ . The velocity condition is the much-used equality form of the Bohm condition.<sup>21</sup> The sheath-liquid interface, which is located at  $z = \xi(x, t)$ , is treated as an equipotential conducting surface with potential  $\phi_{0w}$ . The condition

$$\underline{\hat{n}} \times [\underline{E}]_{z=\xi} = \underline{0}, \quad (4)$$

where the unit normal  $\underline{\hat{n}}$  points into the sheath region, ensures that the electric field remains perpendicular to the liquid surface.

However, the sheath represents only half of the problem; the motion of the conducting liquid, which is taken to be inviscid and incompressible, is determined by

$$\nabla \cdot \underline{v} = 0, \quad (5)$$

$$\rho \frac{\partial \underline{v}}{\partial t} + \rho (\underline{v} \cdot \nabla) \underline{v} + \nabla p = \underline{0}. \quad (6)$$

where  $\underline{v}$ ,  $p$ , and  $\rho$  are the liquid velocity, pressure, and density, respectively. The liquid layer is assumed to be very thick and so its velocity vanishes as  $z \rightarrow -\infty$ . The pressure at the liquid surface is found by considering the forces on a small volume element enclosing the surface. These forces can be expressed in their conservative forms, i.e., as divergences of the stress tensor, which can then be integrated

using the divergence theorem to give the pressure jump condition everywhere on the liquid surface

$$\underline{\hat{n}} p_{z=\xi} + \underline{\hat{n}} \cdot \underline{\sigma}_{z=\xi} + \gamma \kappa \underline{\hat{n}} = \underline{0}. \quad (7)$$

This expression includes the Young-Laplace pressure, with surface tension  $\gamma$  and curvature  $\kappa = -\nabla \cdot \underline{\hat{n}}$ , and the sheath stress tensor

$$\underline{\sigma} = \epsilon_0 \underline{E} \underline{E} - \frac{\epsilon_0 E^2}{2} \underline{I} - m_i n_i \underline{u} \underline{u} - n_s k_B T_e \exp\left(\frac{e\phi}{k_B T_e}\right) \underline{I}, \quad (8)$$

which comprises the electrostatic Maxwell stress, the ion ram pressure, and the electron pressure. Gravity has been neglected in this formulation of the problem; this is valid when  $\gamma k^2 / \rho g \gg 1$  (Ref. 23, Chap. 3) which is easily verified for typical parameters such as those discussed later.

The stability of the plasma-liquid interface is determined according to a standard linearization procedure. First, the equilibrium solution, denoted with a subscripted 0 and corresponding to a static system with its interface at  $\xi_0 = 0$ , is found. All the variables are then separated into zeroth- and first-order terms such as  $\phi = \phi_0 + \phi_1$ , and only the terms which are linear in the first-order quantities are retained in Eqs. (1)–(8). The first-order quantities are assumed to be of the separable form

$$\phi_1 = \tilde{\phi}(z) e^{i(\omega t - kx)}, \quad (9)$$

$$\underline{u}_1 = [\tilde{u}_x(z) \underline{\hat{x}} + \tilde{u}_z(z) \underline{\hat{z}}] e^{i(\omega t - kx)}, \quad (10)$$

etc., where the real part is understood. The interface conditions given by Eqs. (4) and (7) are then applied at the liquid surface defined by

$$\xi_1 = \tilde{\xi} e^{i(\omega t - kx)} \ll \lambda_D, \quad (11)$$

which has the unit normal  $\underline{\hat{n}} = \underline{\hat{z}} + ik \xi_1 \underline{\hat{x}}$ , to give a dispersion relation for  $\omega$ . The height of this perturbation is much smaller than the Debye length,  $\lambda_D$ , which is defined at the plasma-sheath edge. Finally, the marginal stability criterion is found by determining where  $\omega$  transitions from a real, travelling wave solution to an imaginary, exponentially growing solution by setting  $\omega^2 = 0$ .

The zeroth-order planar sheath equations cannot be solved explicitly in terms of  $z$ , but they do permit implicit solutions in terms of the unperturbed electric potential  $\phi_0$ . Equation (2) integrates to give the ion energy conservation equation with the constant of integration given by the sheath-edge Bohm condition and the  $z$ -component of ion velocity follows as:

$$\frac{u_{z0}}{u_B} = - \left( 1 - 2 \frac{e\phi_0}{k_B T_e} \right)^{1/2}. \quad (12)$$

Integration of Eq. (1) gives the ion flux conservation equation and hence

$$\frac{n_0}{n_s} = - \frac{u_B}{u_{z0}} = \left( 1 - 2 \frac{e\phi_0}{k_B T_e} \right)^{-1/2}. \quad (13)$$

The stress balance equation  $\nabla \cdot \underline{\sigma} = 0$ , with  $\underline{\sigma}$  given in Eq. (8), results from a combination of Eqs. (1)–(3) and may be integrated in the planar case to give the electric field

$$\frac{1}{2} \frac{\epsilon_0 E_{z0}^2}{n_s k_B T_e} = \left(1 - 2 \frac{e\phi_0}{k_B T_e}\right)^{1/2} + \exp\left(\frac{e\phi_0}{k_B T_e}\right) - 2. \quad (14)$$

The zeroth-order solutions in the liquid region are simply  $v_0 = \underline{0}$ , and from the pressure jump condition and the uniformity of the  $\sigma_{zz0}$  stress component throughout the sheath,  $p_0 = 2n_s k_B T_e$ .

The zeroth-order sheath solutions allow the immediate derivation of the conventional EHD stability criterion in terms of the plasma and surface properties. Melcher's EHD stability criterion,  $\epsilon_0 E_c^2 = \gamma k$ ,<sup>15</sup> can be written in terms of a critical wall potential using Eq. (14) as

$$\frac{e\phi_c}{k_B T_e} = \frac{1}{2} \left[1 - \left(2 + \frac{k\lambda_D}{2B_{OP}}\right)^2\right], \quad (15)$$

where  $B_{OP} = n_s k_B T_e \lambda_D / \gamma$  is named, by analogy with the electric Bond number,<sup>24</sup> as the plasma Bond number. The critical wall potential tends to  $e\phi_c / k_B T_e = -1/2$  for low-wavenumber perturbations, and this value is always exceeded by the floating potential<sup>25</sup>

$$\frac{e\phi_{0w}}{k_B T_e} = \frac{1}{2} \ln\left(\frac{2\pi m_e}{m_i}\right) \quad (16)$$

of a plasma-facing surface. This might appear to explain the emission of droplets from plasma-liquid interfaces, particularly given that the emission rate is enhanced when large potentials are applied across the sheath,<sup>7</sup> but this analysis neglects the crucial role of the ions which emerge from the following perturbation theory.

The linearized equations in the liquid region are

$$\nabla \cdot v_1 = 0, \quad (17)$$

$$\rho \frac{\partial v_1}{\partial t} + \nabla p_1 = \underline{0}. \quad (18)$$

Taking the divergence of Eq. (18), and inserting Eq. (17), gives a Laplace equation  $\nabla^2 p_1 = 0$  with the solution

$$p_1 = A e^{kz} e^{i(\omega t - kx)} \quad (19)$$

and substitution of this solution into Eq. (18) yields

$$v_1 = A \left( \frac{k}{\omega\rho} \hat{x} + \frac{ik}{\omega\rho} \hat{z} \right) e^{-kz} e^{i(\omega t - kx)}. \quad (20)$$

After linearization, the variables  $\xi_1$  and  $v_{z1}$  are linked by

$$\frac{\partial \xi_1}{\partial t} = v_{z1, z=0} \quad (21)$$

which sets the constant as

$$A = \frac{\omega^2 \rho \tilde{\xi}}{k}. \quad (22)$$

The linearized sheath equations are rather more difficult to solve than those in the liquid region. This set of first-order equations is

$$\frac{\partial \phi_1}{\partial z} = -E_{z1}, \quad (23)$$

$$\frac{\partial \Gamma_{z1}}{\partial z} = ik n_0 u_{x1} - i\omega n_1, \quad (24)$$

$$\frac{\partial u_{x1}}{\partial z} = \frac{ike\phi_1}{m_i u_0} - \frac{i\omega u_{x1}}{u_0}, \quad (25)$$

$$\frac{\partial(u_{z0} u_{z1})}{\partial z} = \frac{e}{m_i} E_{z1} - i\omega u_{z1}, \quad (26)$$

$$\frac{\partial E_{z1}}{\partial z} = \frac{e}{\epsilon_0} \left[ n_1 - \phi_1 \exp\left(\frac{e\phi_0}{k_B T_e}\right) \right] - k^2 \phi_1, \quad (27)$$

where the symbol  $\Gamma_z = nu_z$  represents the flux of ions in the  $z$  direction. All of the first-order sheath quantities tend to zero as  $z \rightarrow \infty$ , while linearization of Eq. (4) gives  $\phi_{1, z=0} = E_{z0, z=0} \xi_1$ .<sup>15</sup> An additional linearization of the  $z$ -component of Eq. (7) yields the first-order pressure jump condition as

$$\frac{\omega^2 \rho}{k} \xi_1 + \sigma_{zz1, z=0} - \gamma k^2 \xi_1 = 0, \quad (28)$$

which provides the dispersion relation of the wave when the value of  $\sigma_{zz1, z=0}$  is known; however, the purpose of this work is to determine the marginal stability condition of the surface perturbations which is the point where  $\omega$  transitions from real to imaginary values, i.e., at  $\omega^2 = 0$ . With this aim in mind, Eqs. (23)–(27) are simplified by removing the  $\omega$  terms, and the condition for instability is given by Eq. (28) with  $\omega$  set equal to zero. Future work will consider the full solutions which retain the  $\omega$  terms.

The perturbed sheath equations require numerical evaluation, even with the  $\omega = 0$  simplification made, and the numerical method is briefly outlined as follows: First, Eq. (26) can be immediately integrated to give  $u_{z1} = -e\phi_1 / m_i u_{z0}$ . Application of the chain rule  $\partial/\partial z = -E_{z0} \partial/\partial \phi_0$  then allows the integration to be performed over a finite domain of  $\phi_0$  values rather than the infinite domain of  $z$  values; this also allows the direct use of the implicit zeroth-order solutions in Eqs. (12)–(14). However, using  $\phi_0$  as the integration variable introduces an irregular point at the sheath edge where  $\phi_0 = 0$ . A Taylor series expansion of Eqs. (23)–(27) at this point proved itself to be extremely difficult to find so an alternative shoot-and-correct method has been developed. This method essentially guesses the values of the perturbed sheath quantities after the first step of the integration and calculates the subsequent steps using the shooting RK4 method until the liquid surface at  $\phi_0 = \phi_{0w}$  is reached. The perturbation to the electric potential is then compared to the boundary condition  $\phi_{1, z=0} = E_{z0, z=0} \xi_1$ , and the initial guessed values are updated accordingly. This cycle of shooting and correcting is continued until the  $\phi_1$  boundary condition is satisfied to within a given error tolerance which was taken to be at least 1 part in  $10^5$ . The codes used to generate and analyse these results are available at <http://www.github.com/joshholgate/ELIPS>.

The solution of the linearized sheath equations gives the  $zz$ -component of the first-order stress tensor at the liquid surface in its normalized form according to

$$\frac{\sigma_{zz1, z=0}}{n_s k_B T_e} = \left[ \frac{\epsilon_0 E_{z0} E_{z1}}{n_s k_B T_e} + \frac{u_{z1}}{u_B} - \frac{u_{z0} \Gamma_{z1}}{n_s u_B^2} - \frac{e\phi_1}{k_B T_e} \right]_{z=0}, \quad (29)$$

which is, of course, a linear function of the surface height perturbation  $\xi_1/\lambda_D$ . Inserting this stress perturbation into Eq. (28) with  $\omega = 0$  gives the marginal stability condition as

$$\frac{\sigma_{zz1,z=0} \lambda_D}{n_s k_B T_e \xi_1} = \frac{k^2 \lambda_D^2}{Bo_P}. \quad (30)$$

The term on the left is computed for various values of surface potential and wavenumber, and Eq. (30) is subsequently solved for different values of  $Bo_P$  in order to find the critical surface potential  $\phi_c$  at which the surface becomes unstable. The results are displayed in Fig. 2.

Two main regimes are observed in Fig. 2. The sloping region towards the right of the plot corresponds exactly to the critical field strength for the EHD instability given earlier by Eq. (15) and displayed as dashed lines. However, this behaviour ceases when, roughly,  $k\lambda_D < 0.1$ , i.e., for plane-wave perturbations with wavelengths longer than around ten Debye lengths. This lengthscale corresponds, intriguingly, to the physical width of a plasma sheath. This departure from the conventional EHD theory indicates that the electric field no longer provides the dominant force on the liquid surface and ion bombardment of the surface can suppress the onset of the EHD instability. The transition between the two regimes is relatively sharp for  $Bo_P \ll 1$  but becomes broader and exhibits a slight dip in the critical surface potential as  $Bo_P$  approaches unity.

The stability criterion can be investigated further by finding the minimum potential which must be applied to the liquid surface in order to make it unstable. These are extracted as the minima of curves such as those in Fig. 2 and are plotted against the plasma Bond number in Fig. 3. The results tend to  $e\phi_c/k_B T_e = -1/2$  for large values of  $Bo_P$  in accordance with the conventional EHD limit given by Eq. (15).

A tokamak edge plasma has electron temperatures of 10–50 eV and densities of  $(0.3\text{--}2) \times 10^{19} \text{ m}^{-3}$ .<sup>26</sup> This plasma may make contact with melted tungsten, with  $\gamma = 2.5 \text{ N m}^{-1}$ , or liquid lithium, with  $\gamma = 0.4 \text{ N m}^{-1}$ , when a liquid divertor is used. These parameters give  $Bo_P$  values of up to  $5 \times 10^{-3}$ ,

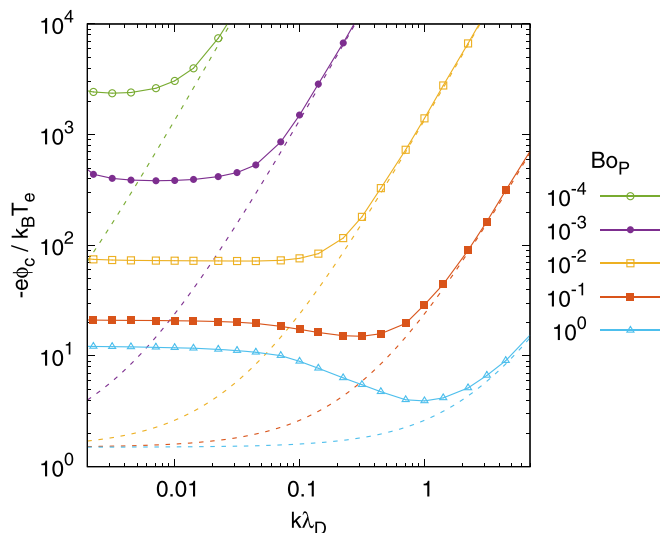


FIG. 2. The critical value of the potential of the liquid surface at which the liquid becomes unstable as a function of wavenumber  $k$  and for a range of plasma Bond numbers  $Bo_P$ . The asymptotic behaviour, Eq. (15), is indicated.

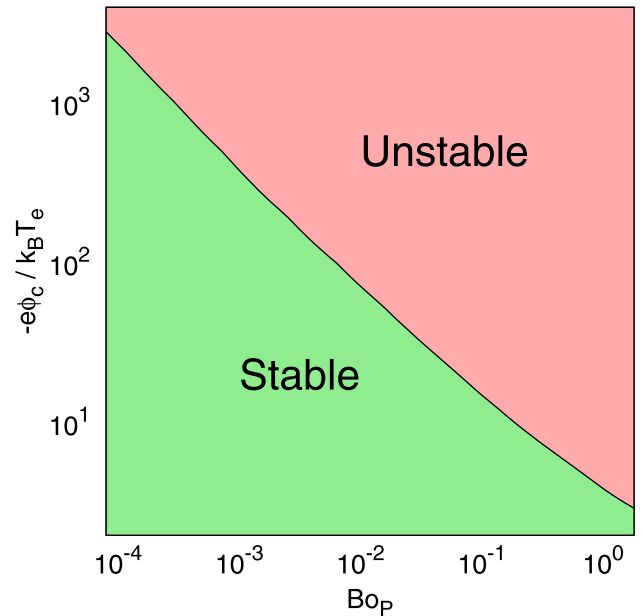


FIG. 3. Plot of the minimum surface potential required to cause the liquid surface to become unstable for each value of  $Bo_P$ . These values are determined by the minimum points of the curves shown in Fig. 2.

and by comparison with Fig. 3, all surfaces with  $-e\phi_{0w}/k_B T_e < 100$  are stable. The floating wall potential of a deuterium plasma, as given by Eq. (16), is  $-e\phi_{0w}/k_B T_e = 3.2$  and so conditions in a tokamak should not lead to an EHD instability. This is a rather unexpected but very useful result; the sheath electric field, according to Eq. (14), exceeds several  $\text{MV m}^{-1}$  which would cause a strong EHD instability if no plasma were present. However, although the sheath alone is insufficient to cause droplet emission, it remains highly plausible that the electric field plays some role in the observation of larger-than-predicted droplets from the bubble-bursting mechanism<sup>12</sup> and the increased emission rate of these droplets from biased surfaces.<sup>7</sup> The theory developed here is not directly applicable to the collisional sheaths of technologically important water cathodes in atmospheric pressure discharges,<sup>2,17</sup> but it suggests that ion bombardment could be exploited to stabilize these interfaces.

In summary, a linear perturbation analysis of a plasma-liquid interface has been presented which fully accounts for the positively charged sheath region between a bulk plasma and an electrically conducting liquid surface. This analysis shows that short-wavelength instabilities behave according to conventional EHD theories, while the growth of long-wavelength perturbations are suppressed by the impact of ions from the plasma on the liquid surface. Liquid metal surfaces under tokamak divertor conditions will be stable against the electric field if a normal sheath is formed, which encourages their further exploitation. This work also advocates further exploration of methods to mitigate EHD instabilities for technologically important atmospheric pressure discharges over water cathodes.

This work was supported by the UK's Engineering and Physical Sciences Research Council and the Imperial College Ph.D. Scholarship Scheme. The code used to generate the results in this paper is available at <http://www.github.com/joshholgate/ELIPS>.

- <sup>1</sup>P. Bruggeman and C. Leys, *J. Phys. D: Appl. Phys.* **42**, 053001 (2009).
- <sup>2</sup>P. J. Bruggeman, M. J. Kushner, B. R. Locke, J. G. E. Gardeniers, W. G. Graham, D. B. Graves, R. C. H. M. Hofman-Caris, D. Maric, J. P. Reid, E. Ceriani, D. Fernandez Rivas, J. E. Foster, S. C. Garrick, Y. Gorbanev, S. Hamaguchi, F. Iza, H. Jablonowski, E. Klimova, J. Kolb, F. Krcma, P. Lukes, Z. Machala, I. Marinov, D. Mariotti, S. Mededovic Thagard, D. Minakata, E. C. Neyts, J. Pawlat, Z. Lj Petrovic, R. Pflieger, S. Reuter, D. C. Schram, S. Schröter, M. Shiraiwa, B. Tarabová, P. A. Tsai, J. R. R. Verlet, T. von Woedtke, K. R. Wilson, K. Yasui, and G. Zvereva, *Plasma Sources Sci. Technol.* **25**, 053002 (2016).
- <sup>3</sup>G. F. Matthews, B. Bazylev, A. Baron-Wiechec, J. Coenen, K. Heinola, V. Kiptily, H. Maier, C. Reux, V. Riccardo, F. Rimini, G. Sergienko, V. Thompson, and A. Widdowson, and JET Contributors, *Phys. Scr.* **T167**, 014070 (2016).
- <sup>4</sup>R. Maingi, S. M. Kaye, C. H. Skinner, D. P. Boyle, J. M. Canik, M. G. Bell, R. E. Bell, T. K. Gray, M. A. Jaworski, R. Kaita, H. W. Kugel, B. P. LeBlanc, D. K. Mansfield, T. H. Osborne, S. A. Sabbagh, and V. A. Soukhanovskii, *Phys. Rev. Lett.* **107**, 145004 (2011).
- <sup>5</sup>G. G. van Eden, T. W. Morgan, D. U. B. Aussems, M. A. van den Berg, K. Bystrov, and M. C. M. van de Sanden, *Phys. Rev. Lett.* **116**, 135002 (2016).
- <sup>6</sup>F. L. Tabarés, *Plasma Phys. Controlled Fusion* **58**, 014014 (2016).
- <sup>7</sup>G. De Temmerman, J. Daniels, K. Bystrov, M. A. van den Berg, and J. J. Zielinski, *Nucl. Fusion* **53**, 023008 (2013).
- <sup>8</sup>P. Fiffis, T. W. Morgan, S. Brons, G. G. van Eden, M. A. Van Den Berg, W. Xu, D. Curreli, and D. N. Ruzic, *Nucl. Fusion* **55**, 113004 (2015).
- <sup>9</sup>G. V. Miloshevsky and A. Hassanein, *Nucl. Fusion* **50**, 115005 (2010).
- <sup>10</sup>M. A. Jaworski, T. Abrams, J. P. Allain, M. G. Bell, R. E. Bell, A. Diallo, T. K. Gray, S. P. Gerhardt, R. Kaita, H. W. Kugel, B. P. LeBlanc, R. Maingi, A. G. McLean, J. Menard, R. Nygren, M. Ono, M. Podesta, A. L. Roquemore, S. A. Sabbagh, F. Scotti, C. H. Skinner, V. A. Soukhanovskii, and D. P. Stotler, and the NSTX Team, *Nucl. Fusion* **53**, 083032 (2013).
- <sup>11</sup>G. A. Mesyats and N. M. Zubarev, *J. Appl. Phys.* **117**, 043302 (2015).
- <sup>12</sup>Y. Shi, G. Miloshevsky, and A. Hassanein, *Fusion Eng. Des.* **86**, 155 (2011).
- <sup>13</sup>M. Laux, M. Balden, and P. Siemroth, *Phys. Scr.* **T159**, 014026 (2014).
- <sup>14</sup>M. Coppins, *Phys. Rev. Lett.* **104**, 065003 (2010).
- <sup>15</sup>J. R. Melcher, *Field-Coupled Surface Waves* (MIT Press, 1963).
- <sup>16</sup>G. I. Taylor and A. D. McEwan, *J. Fluid Mech.* **22**, 1 (1965).
- <sup>17</sup>P. Bruggeman, J. Liu, J. Degroote, M. G. Kong, J. Vierendeels, and C. Leys, *J. Phys. D: Appl. Phys.* **41**, 215201 (2008).
- <sup>18</sup>D. V. Vyalykh, A. E. Dubinov, K. E. Mikheev, Y. N. Lashmanov, I. L. L'vov, S. A. Sadovoi, and V. D. Selemir, *Tech. Phys.* **50**, 1374 (2005).
- <sup>19</sup>J. E. Allen and F. Magistrelli, *Nature* **194**, 1167 (1962).
- <sup>20</sup>N. Shirai, R. Sekine, S. Uchida, and F. Tochikubo, *Jpn. J. Appl. Phys., Part 1* **53**, 026001 (2014).
- <sup>21</sup>D. Bohm, in *The Characteristics of Electrical Discharges in Magnetic Fields*, edited by A. Guthrie and R. K. Wakerling (McGraw-Hill, 1949), Chap. III.
- <sup>22</sup>J. E. Allen, *Plasma Sources Sci. Technol.* **18**, 014004 (2009).
- <sup>23</sup>D. J. Acheson, *Elementary Fluid Dynamics* (Oxford University Press, Oxford, 1990).
- <sup>24</sup>IEEE-DEIS-EHD Technical Committee, *IEEE Trans. Dielectr. Electr. Insul.* **10**, 3 (2003).
- <sup>25</sup>J. E. Allen, "Probe measurements," in *Plasma Physics*, edited by B. E. Keen (IOP Publishing, 1974).
- <sup>26</sup>F. Militello and W. Fundamenski, *Plasma Phys. Controlled Fusion* **53**, 095002 (2011).